Published in final edited form as:
Dev Cell. 2014 November 10; 31(3): 332–344. doi:10.1016/j.devcel.2014.10.005.

SRF regulates craniofacial development through selective recruitment of MRTF cofactors by PDGF signaling

Harish N. Vasudevan[1] and **Philippe Soriano**[1]

[1]Department of Developmental and Regenerative Biology Icahn School of Medicine at Mount Sinai, New York, NY 10029, USA

Summary

Receptor tyrosine kinase signaling is critical for mammalian craniofacial development, but the key downstream transcriptional effectors remain unknown. We demonstrate that SRF is induced by both PDGF and FGF signaling in mouse embryonic palatal mesenchyme cells, and *Srf* neural crest conditional mutants exhibit facial clefting accompanied by proliferation and migration defects. *Srf* and *Pdgfra* mutants interact genetically in craniofacial development, but *Srf* and *Fgfr1* mutants do not. This signal specificity is recapitulated at the level of cofactor activation: while both PDGF and FGF target gene promoters show enriched genome-wide overlap with SRF ChIP-seq peaks, PDGF selectively activates a network of MRTF-dependent cytoskeletal genes. Collectively, our results identify a novel role for SRF in proliferation and migration during craniofacial development and delineate a mechanism of receptor tyrosine kinase specificity mediated through differential cofactor usage, leading to a unique PDGF-responsive SRF-driven transcriptional program in the midface.

Keywords

SRF; PDGF; FGF; MRTF; neural crest; craniofacial development

Introduction

Receptor tyrosine kinases (RTKs) engage shared signaling effectors, such as extracellular signal related kinase (ERK) and phosphatidylinositol 3-kinase (PI3K), but the *in vivo* phenotypes associated with different RTK mutants can be quite distinct (Lemmon and Schlessinger 2010). A central question revolves around how signal specificity arises from a seemingly general set of transduction pathways. At a transcriptional level, RTK signaling classically modulates the expression of immediate early genes (IEGs) (Cochran et al. 1984; Lau and Nathans 1987). While different RTK pathways, such as platelet derived growth factor (PDGF) and fibroblast growth factor (FGF) signaling, induce similar sets of IEGs in

Corresponding author: philippe.soriano@mssm.edu.

cultured cells (Fambrough et al. 1999), genetic experiments in mice suggest a degree of IEG specificity downstream of PDGF signaling (Schmahl et al. 2007). Thus, a major goal remains to characterize the key transcriptional mediators regulated by RTK signaling and determine their specificity downstream of different receptors.

Development of the mammalian face comprises derivatives from all three germ layers, including a unique contribution from the neural crest. Many components of RTK signaling are linked to craniofacial syndromes and phenotypes in both mice and humans (Newbern et al. 2008; Bentires-Alj et al. 2006). Mice harboring neural crest cell (NCC) conditional loss of PDGF receptor α (PDGFRα) using the *Wnt1-Cre* transgene exhibit cleft face and palate (Tallquist and Soriano 2003). Combined loss of both PDGFRα-specific ligands, PDGFA and PDGFC, results in facial clefting (Ding et al. 2004). In humans, mutations in and around PDGFC (Choi et al. 2009; Calcia et al 2013) and PDGFRα (Rattanasopha et al. 2012) have been associated with cleft lip and palate (CL/P), reflecting a conserved role for PDGF signaling in mammalian midface development. Interestingly, NCC conditional loss of FGF receptor 1 (FGFR1) also results in craniofacial defects (Trokovic et al. 2003; Wang et al. 2013), indicating a requirement for both PDGF and FGF signaling in NCCs for craniofacial morphogenesis.

Serum response factor (SRF) is a transcription factor critical for coupling actin dynamics and signaling pathways to gene expression (Posern and Treisman 2006; Olson and Nordheim 2010). SRF was identified as a regulator of the serum response in fibroblasts (Treisman 1987), and more recent work has focused on understanding the mechanisms of SRF specificity at the transcriptional level (Gineitis and Treisman 2001), particularly in regard to interactions with its two major cofactor families: ternary complex factors (TCFs) and myocardin related transcription factors (MRTFs) (Esnault et al. 2014). SRF can be activated in response to many extracellular stimuli, including PDGF and FGF (Treisman 1996; Wang et al. 2004). However, the specificity of SRF activation at a receptor level is unclear, and a direct comparison of SRF function downstream of multiple RTKs has not been carried out.

SRF is essential across many developmental and physiological contexts, including mesoderm formation (Arsenian et al. 1998), cardiac development (Parlakian et al. 2004), angiogenesis (Franco et al. 2008), oligodendrocyte differentiation (Stritt et al. 2009), neuronal migration (Alberti et al. 2005), and circadian regulation (Gerber et al. 2013). SRF was first implicated in neural crest development through an in situ hybridization screen (Adams et al. 2008), and neural crest conditional *Srf* mouse mutants show defects in dorsal root ganglion (DRG) formation (Wickramasinghe et al. 2008), cardiac outflow tract development, and mandible formation (Newbern et al. 2008). No facial clefting phenotypes have been previously reported, and the role of SRF in midface development remains unknown.

In the present study, we report that SRF is required for craniofacial development and responds differentially to PDGF and FGF signaling through selective interactions with MRTF and TCF cofactors. *Wnt1-Cre; Srf*$^{fl/fl}$ mutants exhibit overt facial clefting as well as proliferation and migration deficits in the cranial neural crest and its derivatives. We find

that *Srf* and *Pdgfra* double mutants (*Wnt1-Cre; Srf*$^{+/fl}$*; Pdgfra*$^{+/fl}$) display varying degrees of craniofacial defects, but *Srf* and *Fgfr1* (*Wnt1-Cre; Srf*$^{+/fl}$; *Fgfr1*$^{+/fl}$) do not interact genetically, indicating that SRF function downstream of these two RTKs is not identical. We demonstrate that this specificity is encoded at the level of MRTF-SRF activation and recapitulated in the genome wide binding profile of SRF and MRTF at the promoters of PDGF target genes, particularly those involved in cytoskeletal organization. Taken together, our studies illustrate a novel role for SRF in controlling proliferation and migration during craniofacial development and uncover an example of RTK specificity mediated by a common transcription factor through differential cofactor usage and unique output gene expression signatures.

Results

PDGF activates SRF in MEPMs, and PDGFRα and SRF are coexpressed during craniofacial development

To identify transcriptional targets of PDGF signaling in the midface, RNA-seq was carried out in E13.5 mouse embryonic palatal mesenchyme (MEPM) cells treated with PDGFA (which specifically activates PDGFRα), identifying *Srf* as a PDGF target gene (Table S2, GSE61755). MEPMs express many palatal mesenchyme markers, including *Pdgfra*, and have been used to study PDGF (Fantauzzo and Soriano 2014) and Ephrin signaling (Bush and Soriano 2010). A quantitative PCR (qPCR) timecourse revealed the peak of *Srf* mRNA induction to occur at 60 minutes following PDGF treatment (Fig. 1A), and Western blot confirmed this increase at the protein level (Fig. 1B). The increase in SRF protein prior to *Srf* mRNA is likely due in part to post-transcriptional regulation of IEG induction (Avraham and Yarden 2011). We observed the appearance of a shifted band following PDGF treatment; indeed, SRF is phosphorylated at multiple residues in response to growth factor treatment, and previous work has shown these modifications can affect SRF activity *in vitro* (Rivera et al. 1993; Iyer et al. 2006). Thus, we treated PDGF stimulated MEPM lysates with calf intestinal phosphatase (CIP) which resulted in loss of the upper band (Fig. S1A), indicating PDGF treatment promotes SRF phosphorylation. To determine the signaling dependence of SRF induction, we performed Western blots following PDGF treatment in the presence of PD325901 (MEK inhibitor), LY294002 (PI3K inhibitor), latrunculin B (MRTF inhibitor), and cytochalasin D (MRTF activator). We found that PDGF mediated SRF induction requires both PI3K and ERK signaling as well as MRTF activity (Fig. 1C).

Next, we analyzed the expression pattern of *Srf* and *Pdgfra* during craniofacial development. Whole mount in situ hybridization (WISH) revealed both genes are expressed in the E11.5 medial nasal process (MNP) (Fig. 1D), and we confirmed protein co-expression in the developing MNP and maxillary process (MxP) with anti-SRF immunofluorescence on *Pdgfra*$^{+/GFP}$ reporter embryos (Hamilton et al. 2003) (Fig. S1B). At E13.5, both *Srf* and *Pdgfra* were present broadly in the craniofacial region, with expression noted in the anterior palate at both the mRNA and protein levels (Fig. S1C–D). These experiments show that PDGF induces SRF in an ERK, PI3K, and MRTF dependent manner, and SRF is co-expressed with PDGFRα in the midface.

Srf conditional mutants exhibit overt facial clefting and interact genetically with Pdgfra mutants but not Fgfr1 mutants

While cardiac, neuronal, and mandibular defects have been observed in NCC conditional *Srf* mutants (Newbern et al. 2008; Wickramasinghe et al. 2008), detailed analysis of the craniofacial phenotypes in these mice has not been carried out. We therefore conditionally disrupted *Srf* in NCCs using the *Wnt1-Cre* driver (Danielian et al. 1998). We found fully penetrant facial clefting in *Wnt1-Cre; Srf*$^{fl/fl}$ mutants compared to heterozygous *Wnt1-Cre; Srf*$^{+/fl}$ controls, which appear grossly normal (Fig. 2A–2B′). Further, *Wnt1-Cre; Srf*$^{+/fl}$; *Pdgfra*$^{+/fl}$ double heterozygotes exhibit partially penetrant facial clefting (Fig. 2A″, 2B″), and infrequently recovered *Wnt1-Cre; Srf*$^{fl/fl}$; *Pdgfra*$^{+/fl}$ mutant embryos display even more severe phenotypes characterized by gross midline hemorrhage and blistering in the cephalic region (Fig. 2A‴, 2B‴) (Table S1). The defects observed in *Pdgfra/Srf* double mutants are reminiscent of *Pdgfra*$^{-/-}$ knockouts, which also exhibit facial clefting, hemorrhaging, and blisters (Soriano 1997). We next performed hematoxylin and eosin (H&E) staining, confirming that the facial clefting extends through the midline in both *Wnt1-Cre; Srf*$^{fl/fl}$ and *Wnt1-Cre; Srf*$^{+/fl}$; *Pdgfra*$^{+/fl}$ mutants at E11.5 (Fig. 2C). We carried out morphometric analysis to quantify the relative severity of clefting across genotypes. We found significantly increased distances between the nasal pits (Fig. 2D) as well as reduced maxillary process length (Fig. 2D′) in *Srf* mutants beginning as early as E10.5. No differences in mandibular morphogenesis were detected at these stages (data not shown). Thus, SRF function is required in NCCs for craniofacial development, and *Srf/Pdgfra* compound heterozygotes exhibit phenotypes despite the grossly normal appearance of *Srf* or *Pdgfra* heterozygotes, suggesting these two genes may function within a common network

Given the activation of SRF in response to many extracellular signals (including FGF), we hypothesized that SRF may also function downstream of FGF signaling during craniofacial development. Indeed, FGF stimulation induces *Srf* mRNA in E13.5 MEPMs; however, in contrast to PDGF signaling, FGF mediated SRF induction required ERK signaling but not PI3K or MRTF activity (Fig. S2A–B). Further, no interaction between *Fgfr1* and *Srf* conditional mutants (*Wnt1-Cre; Srf*$^{+/fl}$; *Fgfr1*$^{+/fl}$) was observed (Fig. S2C), despite the fact that FGFR1 is the primary FGF receptor in the neural crest and craniofacial mesenchyme (Trokovic et al. 2003, Park et al. 2008). These results suggest that activation of SRF by PDGF and FGF signaling is fundamentally different, and more broadly, that these two receptors perform at least a subset of non-overlapping functions.

We recently showed that the original *Wnt1-Cre* results in Wnt1 overexpression and enlargement of the midbrain and therefore generated a *Wnt1-Cre*2 transgenic line as an alternative without these caveats (Lewis et al. 2013). Facial clefting phenotypes obtained with this new Cre driver were similar to those observed with the original *Wnt1-Cre* (Fig. S3A).

SRF mutants display cell proliferation and migration deficits during craniofacial development

SRF is known to control a diverse range of cellular outcomes, including cell proliferation, migration, survival, and differentiation. Thus, we examined each of these processes in *Wnt1-*

Cre; Srf$^{fl/fl}$ mutants to determine the basis for the observed clefting phenotypes. We found reduced proliferation in the MNP of *Srf* mutants (Fig. 3A–B″) at both E10.5 and E11.5. Similarly, we found fewer cells specifically in the MNP of E11.5 *Wnt1-Cre; Srf*$^{fl/fl}$ mutant embryos (Fig. 3C) although no such reduction in total cell number was observed at E10.5 (data not shown). This spatiotemporally specific proliferation defect in *Wnt1-Cre; Srf*$^{fl/fl}$ mutants is consistent with previous work showing that *Wnt1-Cre; Pdgfra*$^{fl/fl}$ mutants also exhibit reduced MNP proliferation (He and Soriano 2013). We did not find any difference in apoptosis between control and *Srf* mutant embryos in the MNP or LNP, and we did not detect any change in the expression of MNP marker genes, such as *Alx3* (data not shown).

Classic studies have shown that many craniofacial structures are predominantly derived from the neural crest (Couly et al. 1993; Chai et al. 2000). To visualize defects in migration and population of the craniofacial mesenchyme by NCCs, we crossed *Srf* conditional mutants to *R26R*-lacZ mice (Soriano 1999). At E9.5, *Wnt1-Cre; Srf*$^{fl/fl}$; *R26R*$^{+/-}$ mutant embryos showed impaired neural crest contribution to the frontonasal prominence (FNP), first branchial arch (BA1), and second branchial arch (BA2) (Fig. 3D–E). We often observed BA1 and BA2 defects in early E9.5 embryos (<18 somites, 7/9 mutant embryos with phenotype) and FNP and BA2 defects in late E9.5 embryos (≥18 somites, 6/9 mutant embryos with phenotype). The combination of lineage tracing and proliferation defects reflects the requirement of SRF activity in the neural crest to both fully populate the craniofacial mesenchyme and respond to proliferative signals.

SRF is required for cellular responses to RTK signaling in facial prominence cells

Since *Wnt1-Cre; Srf*$^{fl/fl}$ embryos are recovered below Mendelian ratios at E13.5, we turned to an earlier stage of craniofacial development to further investigate SRF function. Given the *in vivo* defects observed in the E11.5 midface, we established facial prominence cells (FPCs) from E11.5 embryos as a primary cell culture model to study the effects of SRF loss; control FPCs show robust expression of *Srf*, *Pdgfra*, and *Fgfr1*, and *Wnt1-Cre*2; *Srf*$^{fl/fl}$ mutant FPCs express almost no *Srf* mRNA (Fig. S3B) or protein (Fig. S3C).

SRF is critical for maintaining proper cytoskeletal morphology (Schratt et al. 2002). Thus, we stained *Srf* mutant FPCs for F-actin and β-tubulin and observed gross defects in actin stress fiber formation and microtubule organization (Fig. 4A). Next, we tested the proliferative response of FPCs to PDGF and FGF stimulation. Surprisingly, only PDGF induced proliferation in control FPCs while *Srf* mutant FPCs fail to proliferate following PDGF treatment, reflecting the requirement of SRF function for PDGF-dependent cell proliferation (Fig. 4B). The selective response of FPCs to PDGF may partially explain the phenotypic interactions observed between *Srf* and *Pdgfra* conditional mutants but not *Srf* and *Fgfr1* conditional mutants. Finally, we performed scratch assays to compare the response of control and *Srf* mutant FPCs. In *Wnt1-Cre*2; *Srf*$^{+/fl}$ FPCs, 10% FBS, PDGF, and FGF all induced significant wound closure, but this response was abrogated under all conditions in *Wnt1-Cre*2, *Srf*$^{fl/fl}$ mutant FPCs, reflecting an intrinsic defect in *Srf* mutant cells (Fig. 4C, Fig. S3D). Knockdown of SRF is crucial for both cell motility and directional persistence (Medjkane et al. 2009), and we therefore performed time-lapse microscopy and single cell tracking to better understand this deficit. These experiments revealed that

although a subset of *Wnt1-Cre*2; $Srf^{fl/fl}$ mutant FPCs do move efficiently (Fig. 4D, Fig. S3E), *Srf* mutant FPCs overall are significantly slower and exhibit decreased directional persistence compared to control cells (Fig. 4E). In sum, *Wnt1-Cre*2; $Srf^{fl/fl}$ FPCs display proliferation and motility defects in response to growth factor stimulation, linking the observed *in vivo* proliferation and lineage tracing defects in *Srf* mutants to RTK signaling and demonstrating the functional relationship between these pathways in the midface.

PDGF mediates MRTFA-SRF complex formation and uniquely activates a set of MRTF-SRF associated cytoskeletal genes

In addition to direct transcriptional induction, many mechanisms have been described to regulate SRF function, including alternative splicing (Belaguli et al. 1999), direct nuclear translocation (Camoretti-Mercado et al. 2000), and differential cofactor usage (Posern and Treisman 2006). Therefore, we investigated how these parameters are modulated by RTK activation and whether signal specificity was encoded through these mechanisms. We did not detect alternative splicing of SRF (Fig. S4A–C), and PDGF treatment did not significantly alter the cellular localization of SRF in MEPMs (Fig. S4D). Similarly, we did not observe changes in SRF splicing or localization following FGF treatment (data not shown), suggesting these mechanisms are not utilized by either RTK in this context.

The two major cofactor families utilized by SRF are the TCFs (Elk1, Elk3/Net, and Elk4/Sap1) and MRTFs (MRTFA/Mkl1 and MRTFB/Mkl2). MRTF-dependent SRF activity occurs downstream of changes in actin concentration predominantly mediated by Rho-family small GTPases (Miralles et al. 2003; Vartiainen 2007). In contrast, TCF-dependent SRF activation lies downstream of ERK signaling (Posern and Treisman 2006). The distinction between the two mechanisms of SRF activation has a functional consequence, as unique SRF regulated gene sets are controlled through each of these pathways (Gineitis and Treisman 2001). Although RTK signaling is traditionally associated with robust activation of ERK, PDGF and FGF have also been shown to modulate small GTPase function in many contexts, including the midface (He and Soriano 2013). We began by screening the expression of SRF cofactor genes in MEPM RNA-seq and published E13.5 palate RNA-seq data (www.facebase.org, accession FB00000278.2); only *Elk1*, *Elk3*, and *Mrtfa* are expressed above a FPKM threshold of 10 in both datasets (Fig. 5A). We next performed WISH in E11.5 embryos to determine the expression pattern of these cofactors and compared them to *Srf* and *Pdgfra*. Both *Elk1* and *Elk3* show strong expression in the MNP, but *Mrtfa* is also expressed throughout the craniofacial region, albeit more diffusely (Fig. 5B). Thus, based on expression pattern alone, any of these cofactors may synergize with SRF in the midface.

In order to directly test SRF-cofactor complex formation, we treated E13.5 MEPMs with either PDGF or FGF, performed immunoprecipitation (IP) for either Elk1 or MRTFA, and then Western blotted for SRF. Although both PDGF and FGF promoted formation of an SRF-Elk1 complex, only PDGF treatment resulted in SRF-MRTFA association; conversely, FGF stimulation reduced the amount of SRF-MRTFA complex (Fig. 5C, Fig. S4E). This PDGF mediated SRF-MRTFA association required PI3K (Fig. 5D) activity while SRF-Elk1 association required both ERK and PI3K signaling (Fig. S4E), consistent with previous

work implicating PI3K as the key effector of PDGFRα signaling during craniofacial development (Klinghoffer et al. 2002; Fantauzzo and Soriano 2014). Since MRTF activation results in shuttling of the protein from the cytoplasm to the nucleus (Miralles et al. 2003), we next performed MRTFA immunofluorescence in MEPMs (Fig. 5E). While MRTFA is predominantly cytoplasmic in starved cells, PDGF stimulation increases nuclear MRTFA. FGF also induces MRTFA translocation, but to a lesser extent than PDGF. Indeed, PDGF induced MRTFA shuttling occurs at comparable ratios to cytochalasin D treated MEPMs, consistent with a full MRTFA response to PDGF. The observed heterogeneity of the MRTFA response in MEPMs may be in part a result of our primary cell culture system, and quantitatively similar changes in nuclear MRTFA have been observed in other studies (Ho et al. 2013).

These results raised the possibility that PDGF signaling preferentially drives MRTFA dependent SRF activity while both PDGF and FGF activate Elk1 mediated SRF function. In order to gain insight toward the genome wide role of SRF downstream of these pathways, we integrated our MEPM RNA-seq data with SRF chromatin immunoprecipitation (ChIP) sequencing data from mouse C2C12 (ENCODE 2012; GSM915168) and 3T3 (Esnault et al. 2014) cells. Although SRF binding events are unlikely to be fully conserved across different contexts, a previous study estimated ~60% of SRF binding events in the proximal promoter are shared between cell types (Sullivan et al. 2011), supporting our correlative approach. We also recently generated an analogous RNA-seq dataset for FGF treated MEPMs, allowing comparison of the transcriptional outputs from both PDGF and FGF signaling (Table S2). First, we plotted the distribution of SRF ChIP-seq peaks from the transcriptional start site (TSS) of all genes upregulated at one hour by either PDGF (125 significant genes) or FGF (135 significant genes) (Fig. 6A–B). We found enrichment of SRF ChIP-seq peaks upstream from the TSS of RTK regulated genes, suggesting SRF mediated transcription plays a key role in the genome-wide response to both PDGF and FGF. A full list of these peaks and genes is provided (Table S3). No such enrichment was observed in randomly selected, expression matched control genes (Fig. 6A–B, black lines) unresponsive to growth factor treatment or when plotting the peak distribution from ChIP-seq data for Jun (induced upon PDGF treatment in MEPMs), Pax5 (not expressed in MEPMs), or p300 (a transcriptional co-activator sampled in the E13.5 palate) (Fig. S5A–C).

A total of 94 PDGF and 95 FGF target genes contain an SRF ChIP-seq peak within 70 kb of the TSS in either C2C12 or 3T3 cells; over half of these genes are induced by both pathways (56% shared) (Fig. 6C). Many classic IEGs (such as *Fos*, *Jun*, and *Egr*) fall into the group of 53 genes with SRF binding events that are jointly induced by both PDGF and FGF signaling. Interestingly, a high percentage of genes (56–75%) were conserved in both ChIP-seq datasets (Table S3). Gene ontology analysis revealed that PDGF-responsive SRF targets show overrepresentation of genes associated with the actin cytoskeleton while FGF-mediated SRF targets show no such relationship (Fig. 6D). To visualize these target genes at the level of cofactor specificity, we next integrated our datasets with recently published MRTF and TCF ChIP-seq datasets in 3T3 cells that assigned a score for each target gene reflecting the relative binding of these cofactors (Esnault et al. 2014) (Table S4). We found that many shared RTK targets possess high TCF scores, but a subset of PDGF specific genes

show high MRTF scores (Fig. S5D–E). Indeed, MRTF scores for PDGF-SRF target genes are significantly increased compared to MRTF scores or FGF-SRF target genes (Fig. 6E), but no such difference is observed for TCF scores (Fig. S5F). This correlation between PDGF target genes and SRF-MRTF binding genome-wide may reflect a PDGF-MRTF-SRF circuit not regulated by FGF signaling.

SRF regulates the expression of a cytoskeletal network critical for craniofacial development

Our genomic analyses suggest PDGF mediated SRF activation results in activation of a key cytoskeletal transcriptional program; however, given the ChIP-seq and RNA-seq data were generated from different cell types, our correlative approach alone does not delineate whether these binding events and gene expression changes are functional. Thus, we probed this network in more detail using a candidate-based approach. We selected eight genes for further study based on published mouse craniofacial phenotypes and reported disease associations in humans (Fig. S6A). Many of these genes show high MRTF scores and, in the case of *Acta1* and *Myh9*, have been previously identified as MRTF target genes (Sun et al. 2006; Medjkane et al. 2009). We performed endogenous SRF ChIP in E13.5 MEPMs at previously identified SRF binding sites in these eight target promoters, finding six (*Vcl, Acta2, Myh9, Actb, Tgln, Flna*) to show SRF binding (Fig. S6B). Five of these six promoters (*Acta2, Vcl, Myh9, Actb, Flna)* exhibit increased SRF binding following PDGF stimulation; comparing the two RTKs, all six targets show significantly greater SRF binding in response to PDGF, while only one promoter (*Actb)* exhibits increased binding following FGF stimulation (Fig. 6F). In contrast, SRF binding at the promoter of the shared target *Fos* is induced by both PDGF and FGF signaling, and low occupancy was observed in the promoter of *Arid5b*, an IEG not bound by SRF in either ChIP-seq dataset (Fig. S6C).

Given the importance of PI3K signaling downstream of PDGF in the midface, we assayed the effect of PI3K inhibition on SRF binding. We found decreased PDGF mediated SRF binding at all six targets following pretreatment with LY294002; however, two target promoters (*Acta2* and *Actb*) still showed significant responses, indicating PI3K signaling is not always required for SRF binding (Fig. 6F). In addition, PI3K inhibition significantly decreased SRF binding at the *Tagln* promoter across all conditions, suggesting PI3K promotes SRF maintenance at this locus. Next, we carried out endogenous MRTFA ChIP and demonstrate significantly increased MRTFA binding at four loci (*Acta2, Vcl, Myh9, Actb)* in response to PDGF treatment (Fig. 6F). In contrast, FGF induced significant MRTFA binding at only the *Actb* promoter, consistent with the increased SRF binding at this region. No MRTFA binding was observed at either the *Flna* or *Fos* (Fig. S6C) promoter. Collectively, these results indicate PDGF and FGF differentially modulate SRF and MRTFA binding at target gene promoters, in part through PI3K signaling.

To determine the MRTF dependence of these genes, we stimulated MEPMs with PDGF or FGF in the presence of Latrunculin B (Fig. 7A). All six genes are selectively induced by PDGF. Further, Latrunculin B inhibits the PDGF mediated expression of five genes (*Acta2, Vcl, Myh9, Actb, Tagln),* confirming these targets are indeed MRTF dependent. While MRTFA nuclear accumulation is observed at 30 minutes following PDGF treatment, both

the repressive effect of Latrunculin B and observed MRTFA binding at target gene promoters is more pronounced at four hours, suggesting MRTF mediated changes in gene expression may be a delayed response. The induction of *Fos* by both PDGF and FGF is not affected by Latrunculin B (Fig. S6D). We then measured the expression of these six genes in E11.5 facial prominences (MNP, LNP, and MxP) dissected from *Srf*, *Pdgfra*, and *Fgfr1* conditional mutants. As expected, the expression of *Srf*, *Pdgfra*, and *Fgfr1* were decreased in the corresponding mutants; further, we observed downregulation of all six targets in *Srf* mutant facial prominences (Fig. 7B). Finally, we found significantly decreased expression of four PDGF-SRF targets (*Vcl*, *Myh9*, *Actb*, and *Flna)* in *Pdgfra* mutants, but not *Fgfr1* mutants (Fig. 7B). Interestingly, a modest increase in *Pdgfra* expression was observed in *Srf* mutants, possibly indicating a compensatory feedback mechanism. These results reflect the perturbation of a PDGF responsive, MRTF dependent cytoskeletal circuit specifically in *Pdgfra* and *Srf* mutants.

Our data suggest the following model: PDGF mediates MRTFA-SRF association and binding at select target gene promoters to drive MRTF dependent expression of key actomyosin cytoskeleton elements (such as *Vcl*, *Actb*, *Acta2*, and *Myh9)*. In contrast, both PDGF and FGF signaling increase Elk1-SRF complex formation to modulate the classic IEG signature (including *Fos*, *Fosb*, and *Junb*) observed downstream of these pathways. By building a protein-protein interaction (PPI) network of the targets downstream of PDGF, FGF, and SRF (Chen et al. 2012), we can better visualize this specificity at both the RTK and cofactor levels (Fig. 7C). Consistent with our framework, the PDGF specific PPI network shows strong correlation with MRTF target genes. Our studies imply that loss of this PDGF-MRTF-SRF axis explains in part both the craniofacial phenotypes of *Pdgfra* and *Srf* conditional mutants as well as the observed phenotypic interaction between these two genes.

Discussion

SRF is a classic regulator of the transcriptional response to growth factor signaling. In the present study, we find that neural crest conditional loss of SRF results in facial clefting accompanied by proliferation and migration defects. By analyzing SRF activation downstream of both PDGF and FGF signaling, we uncover a PDGF-MRTF-SRF circuit critical for cytoskeletal gene expression in the midface. We conclude that SRF is required for craniofacial development, and RTK signaling encodes the specificity of SRF mediated gene expression at the level of cofactor recruitment in this developmental context.

Many phenotypes have been reported in SRF neural crest conditional mutants (Newbern et al. 2008, Wickramasinghe et al. 2008), and we now describe gross facial clefting in these mutants, which had not been previously appreciated. We further demonstrate SRF drives proliferation of the NCC derived MNP mesenchyme. MNP cell proliferation is also decreased in *Wnt1-Cre; Pdgfra*$^{fl/fl}$ mice (He and Soriano 2013), suggesting a common mechanism underlying both PDGF and SRF activity. Consistent with this notion, SRF mutant FPCs fail to proliferate in response to PDGF stimulation. Thus, PDGF signaling acts through SRF to drive a functional proliferation program in the midface. In the epidermis, loss of *Srf* leads to cell proliferation defects due to abnormalities in the actomyosin network

(Luxenburg et al. 2011); many targets of the PDGF-MRTF-SRF axis elucidated in our study (such as *Actb, Myh9, Flna,* and *Actg1*) were also implicated in the proliferation defects observed in these epidermis-specific *Srf* mutants, reflecting the importance of these genes. We further show that *Wnt1-Cre; Srf*$^{fl/fl}$ embryos exhibit lineage tracing defects characterized by decreased infiltration of NCCs into the FNP and first two branchial arches, raising the possibility that the facial clefting may be in part the result of an insufficient number of neural crest derived progenitors populating the craniofacial mesenchyme. To understand the basis for these deficits, we analyzed SRF deficient primary cells isolated from the cranial NCC derived facial prominences and demonstrated decreased speed and directional persistence in wound healing assays. Upon delamination from the dorsal neural tube, neural crest cells migrate in stereotypic streams throughout the embryo to populate a diverse range of derivatives, responding to guidance cues as they migrate collectively to their final destinations (Theveneau and Mayor 2012). Many PDGF regulated SRF target genes in our study are involved in force generation (*Myh9, Myl6, Myl12b*), focal adhesion formation (*Vcl, Flna, Zyx*) and cytoskeletal organization (*Actb, Actg1, Acta2*), key processes for cell migration. In addition, MRTFs have been shown to mediate cell motility and directionality in other contexts (Medjkane et al. 2009), suggesting the observed defects may be MRTF-dependent.

Upon activation, RTKs become phosphorylated and engage downstream effectors, which in turn activate many shared intracellular pathways. One outcome of this signaling cascade is the transcription of IEGs. Many RTKs induce overlapping sets of IEGs, leaving open the question of how transcriptional specificity is generated. We demonstrate that PDGF, but not FGF, selectively promotes recruitment of SRF and MRTFA to target gene promoters, leading to induction of a unique gene expression program. This PDGF-MRTF-SRF axis is enriched for cytoskeletal regulators, many of which exhibit MRTF dependent induction and decreased expression in *Srf* and *Pdgfra* mutants. On the other hand, both PDGF and FGF increase Elk1-SRF complex formation, in line with our observation that over half of the identified SRF target genes are jointly activated by both PDGF and FGF. The targets downstream of this shared RTK-Elk1-SRF axis, such as *Fos, Jun,* and *Egr,* comprise a classic set of IEGs activated by multiple pathways (Fambrough et al. 1999), suggesting other stimuli can compensate for loss of Elk1-SRF mediated transcription. Consistent with this notion, *Srf* null embryos express residual amounts of *Fos* and *Egr1* but show complete loss of *Acta1* expression (Arsenian et al. 1998). We propose that the PDGF-MRTF-SRF axis has unique roles in the developing midface, an assertion supported by our epistasis results and gene expression studies.

Two critical points merit further discussion. First, what are the key signaling parameters encoding differential cofactor activation and SRF-mediated gene expression downstream of PDGF and FGF signaling? A potential answer lies in the importance of PI3K activity in the formation of an MRTFA-SRF complex and in driving maximal SRF binding at target gene promoters in response to PDGF stimulation. Previous studies have shown PI3K to be the primary effector downstream of PDGF signaling during midface development, closely mirroring the craniofacial phenotypes observed in PDGFRα mutants (Klinghoffer et al. 2002; Fantauzzo and Soriano 2014). Thus, one explanation is that PDGF activated PI3K

signaling selectively promotes MRTFA-SRF association, perhaps through Rho-family small GTPases, which modulate actin dynamics and MRTF activity in other contexts (Pipes et al. 2006). Both Rac1 and Cdc42 are required in the neural crest for craniofacial development (Thomas et al. 2010; Fuchs et al. 2009) and have been implicated downstream of PDGF signaling in MEPMs (He and Soriano 2013; Fantauzzo and Soriano 2014). Although FGF signaling can modulate both Rac1 and Cdc42 in other systems (Fera et al. 2004; Clark et al. 2011), it is unclear whether this relationship is conserved in the midface. Alternatively, while both PDGF and FGF signal through common kinase cascades, the magnitude and duration of this induction can be quite different. Indeed, PDGF and FGF mediated pERK activation patterns are markedly different in MEPMs, with PDGF stimulation resulting in a transient pERK pulse but FGF treatment driving sustained pERK activation (unpublished data). Consistent with this observation, a recent study showed that sporadic pERK pulses drive SRF mediated transcription more efficiently than sustained pERK activity (Aoki et al. 2013), reflecting yet another layer of control. In sum, a combination of both qualitative and quantitative differences in signaling parameters likely accounts for the observed SRF specificity.

Second, is this specificity of SRF activation ‘hard-wired’ into the PDGF and FGF signaling networks or is it context dependent? The answer is almost certainly the latter, as the magnitude and kinetics of activation downstream of even the same RTK can vary depending on many parameters, including expression level (Traverse et al. 1994). The expression pattern of many signaling components is restricted over the course of development, necessitating diverse, context-specific control systems. The neural crest itself is a multipotent population with many sublineages, all expressing different combinations and amounts of receptors and signaling effectors. In the case of PDGFRα and SRF, we describe a PDGF-SRF circuit in the midface. However, many of the observed hemorrhaging and blistering phenotypes in these mutants may be due in part to requirements for PDGF signaling and SRF activity in neural crest derived vascular components, such as smooth muscle cells and pericytes (Etchevers et al. 2001). The PDGF-SRF signaling axis may be wired differently in these cells, particularly at the levels of receptor activation, effector requirements, and cofactor recruitment. In DRG sensory neurons, SRF activity downstream of nerve growth factor (NGF) is dependent on ERK mediated MRTFA activity, but not on TCF-SRF complex formation (Wickramasinghe et al. 2008). Thus, SRF function can be controlled by different RTKs in divergent neural crest lineages through a common set of cofactors and signaling effectors. The degree of sophistication and stimulus-dependent utilization of SRF regulatory mechanisms is remarkable, and determining the exact rules governing SRF activity following receptor activation across these diverse developmental contexts will be rewarding. Our studies provide one such example of the intricate control systems in place to encode transcriptional specificity downstream of two different RTKs at the level of SRF cofactor recruitment.

Experimental Procedures

Mouse strains

All animal experiments were approved by the Institutional Animal Care and Use Committee at the Icahn School of Medicine at Mount Sinai. *Srf*^{tm1Rmn} mice (Ramanan and Ginty 2005) referred to as *Srf*$^{fl/fl}$ in the text, were a gift from Dr. Xin Sun, University of Wisconsin-Madison, and were backcrossed a minimum of three generations to 129S4 mice prior to all experiments included in this study. *Tg*(*Wnt1-Cre*)*2Sor* mice (Lewis et al. 2013), referred to as *Wnt1-Cre*2 in the text, were backcrossed to 129S4 mice for four generations prior to all experiments in this study. *Pdgfra*$^{tm11(EGFP)Sor}$ (Hamilton et al. 2003), referred to as *Pdgfra*$^{GFP/+}$ in the text, and *Gt(ROSA)26Sor*^{tm1Sor} mice (Soriano 1999), referred to as *R26R* in the text, were maintained on a C57BL/6 background. *PDGFRα*^{tm8Sor} mice (Tallquist and Soriano 2003), referred to as *Pdgfra*$^{fl/fl}$, in the text, *FGFR1*$^{tm5.1Sor}$ mice (Hoch and Soriano 2006), referred to as *Fgfr1*$^{fl/fl}$ in the text, and *Tg(Wnt1-Cre)11Rth* mice (Danielian et al. 1998), referred to as *Wnt1-Cre* in the text, were all maintained on a 129S4 genetic background.

Tissue culture and proliferation/scratch assays

Primary mouse embryonic palatal mesenchyme (MEPM) cells were isolated from E13.5 secondary palatal shelves (day of plug: E0.5) as previously described (Fantauzzo and Soriano 2014). Primary mouse facial prominence cells (FPCs) were generated from E11.5 mouse facial prominences (Fig. S3B), but we were unable to passage these FPCs in culture. Therefore, MEPMs were used for further experiments investigating RTK mediated control of SRF function, such as Western blots and ChIP. For proliferation assays, cells were starved overnight and then incubated with 10 μm BrdU for 4 hours (Bush and Soriano 2010) with either 30 ng/mL PDGFAA or 50 ng/mL FGF1 + 1 μg/mL heparin. For wound healing assays, cells were grown to confluence, starved overnight, and then scratched. Details are available in Supplemental Procedures.

Histology, *In situ* hybridization, and Immunofluorescence

Embryos were dissected and embedded in either paraffin or optimal cutting temperature (OCT) compound for sectioning. *In situ* hybridization and immunofluorescence were performed according to standard protocols. See Supplemental Procedures for further details.

qPCR

For analysis of SRF induction, E13.5 MEPMs were starved overnight and then treated with PDGF or FGF for the desired time duration. For analysis of SRF target gene expression in mutant embryos, E11.5 facial prominence lysates were harvested and RNA was extracted directly from tissue. All experiments were conducted on litters from three independent biological replicates. Statistical analysis was performed using a two-tailed, paired Student's t-test for MEPM timecourses, in which cells from the same embryo were considered paired. For comparison of expression between facial prominence lysates from different genotypes, a two-tailed, unpaired Student's t test was used. Further details are available in Supplemental Procedures.

Time lapse imaging

FPCs were prepared and scratch assays performed as described above. Live cell imaging was carried out on an Olympus IX-70 widefield epi-fluorescence system with a stage-top incubation chamber to maintain cell viability. Images were taken with a 10x lens every 5 minutes across 250 minutes, for a total of 50 images per field of view. Four fields of view per condition per embryo were imaged, and two independently dissected control and mutant embryos were analyzed. Ten cells were randomly selected in each field of view for tracking and calculation of migration parameters, and thus, a total of 40 cells per condition per embryo were analyzed. Image analysis was performed in ImageJ (v 1.47; NIH, Bethesda, MD, USA) using the Manual Tracking plugin. Calculation of trajectories, speed and persistence were implemented through custom code in R (www.R-project.org/).

IP and Western blot

E13.5 MEPMs were serum starved for 24 hours in 0.1% FBS and stimulated with PDGF or FGF for desired duration. When applicable, cells were pretreated for 1 hr with 10 μM of desired inhibitor. IPs and Western blots were performed according to standard protocols using HRP-conjugated secondary antibodies and quantified in ImageJ (v 1.47; NIH, Bethesda, MD, USA). A minimum of two biological replicates were performed for each set of IP experiments. Further details are provided in Supplemental Procedures.

ChIP

E13.5 MEPMs were isolated and stimulated with PDGF or FGF as described above. ChIP was performed as previously described (Fantauzzo and Soriano 2014) to test occupancy in input, IgG, and antibody (anti-SRF or anti-MRTFA) precipitated samples. qPCR was carried out as described above, and statistics were performed using a two-tailed, paired Student's t-test, in which cells from the same embryo were considered paired. Data presented are from three independent biological replicates. Further details are provided in Supplemental Procedures.

ChIP-seq and RNA Seq data integration

C2C12 SRF ChIP-seq peak data was downloaded directly from the ENCODE consortium (www.encodeproject.org; GEO GSM915168) in the 'narrowPeaks' format, which lists significant peaks identified by the ENCODE consortium. 3T3 SRF ChIP-seq data was similarly obtained (Esnault et al. 2014). Chromosomal coordinates for each of these peaks were then compared to the transcriptional start site (TSS) for each gene regulated by PDGF or FGF signaling at 1 hour, and a frequency distribution was generated by counting the number of peaks within successive 10kb bins of the TSS. Strategy was implemented through custom code in R. Similar distributions for control gene sets (randomly selected, expression matched genes that are not regulated by RTK activation) were generated to assess baseline ChIP-seq peak enrichment. A similar approach was implemented for the following control ChIP-seq datasets:

1. Jun (GEO: GSM9212901)
2. Pax5 (GEO: GSM923584)

3. E13.5 palate p300 (www.facebase.org; Accession FB00000263)

Supplementary Material

Refer to Web version on PubMed Central for supplementary material.

Acknowledgments

We are very grateful to Fenglei He for performing the initial RNA-seq experiment. We thank Jason Newbern at the University of North Carolina for discussion on SRF mutant phenotypes. *Srf*$^{fl/fl}$ mice were a gift from Dr. Xin Sun at the University of Wisconsin-Madison. Excellent genotyping and technical support were provided by Tony Chen, Aryel Heller, and Anne Levine. Live imaging was performed in the Microscopy Shared Resource Facility at the Icahn School of Medicine at Mount Sinai, and we thank Rumana Huq and Lauren O'Rourke for assistance. RNA-seq experiments were performed at the Mount Sinai Genomics Core, and we thank Omar Jabado, Yumi Kasai, Milind Mahajan, and Avi Ma'ayan for advice and discussions. We are grateful to the Developmental Studies Hybridoma Bank for reagents. ENCODE ChIP-seq datasets were downloaded for SRF (Wold lab), Jun (Snyder lab) and Pax5 (Hardison lab). FaceBase datasets were downloaded for E13.5 palate p300 ChIP-Seq and E13.5 palate RNA-seq (Visel lab). We thank Robert Krauss, Susan Parkhurst, and the members of the Soriano laboratory for helpful discussion and critical comments on this manuscript. This work was supported by NIH/NIDCR grants R01DE022363 and R01DE022778 to P.S. and NIH/NIDCR Ruth L. Kirschstein NRSA Individual Predoctoral Fellowship F31DE023456 to H.N.V.

References

Adams MS, Gammill LS, Bronner-Fraser M. Discovery of transcription factors and other candidate regulators of neural crest development. Dev Dynamics. 2008; 237:1021–33.

Alberti S, Krause SM, Kretz O, Philippar U, Lemberger T, Casanova E, Wiebel FF, Schwarz H, Frotscher M, Schutz G, Nordheim A. Neuronal migration in the murine rostral migratory stream requires serum response factor. PNAS. 2005; 102:6148–6153. [PubMed: 15837932]

Aoki K, Kumagai Y, Sakurai A, Komatsu N, Fujita Y, Shionyu C, Matsuda M. Stochastic ERK Activation Induced by Noise and Cell-to-Cell Propagation Regulates Cell Density-Dependent Proliferation. Mol Cell. 2013; 52:529–540. [PubMed: 24140422]

Arsenian S, Weinhold B, Oelgeschläger M, Rüther U, Nordheim A. Serum response factor is essential for mesoderm formation during mouse embryogenesis. EMBO Journal. 1998; 17:6289–99. [PubMed: 9799237]

Avraham R, Yarden Y. Feedback regulation of EGFR signalling: decision making by early and delayed loops. Nat Rev Mol Cell Bio. 2011; 12:104–17. [PubMed: 21252999]

Belaguli NS, Zhou W, Trinh TH, Majesky MW, Schwartz RJ. Dominant negative murine serum response factor: alternative splicing within the activation domain inhibits transactivation of serum response factor binding targets. Mol Cell Bio. 1999; 19:4582–91. [PubMed: 10373507]

Bentires-Alj M, Kontaridis MI, Neel BG. Stops along the RAS pathway in human genetic disease. Nature Medicine. 2006; 12:283–285.

Bush JO, Soriano P. Ephrin-B1 forward signaling regulates craniofacial morphogenesis by controlling cell proliferation across Eph-ephrin boundaries. Genes & Dev. 2010; 24:2068–80. [PubMed: 20844017]

Calcia A, Gai G, Di Gregorio E, Talarico F, Naretto VG, Migone N, Pepe E, Grosso E, Brusco A. Bilaterally cleft lip and bilateral thumb polydactyly with triphalangeal component in a patient with two de novo deletions of HSA 4q32 and 4q34 involving PDGFC, GRIA2, and FBXO8 genes. American Journal of Med Gen. 2013; 161:2656–62.

Camoretti-Mercado B, Liu HW, Halayko J, Forsythe SM, Kyle JW, Li B, Fu Y, McConville J, Kogut P, Vieira JE, et al. Physiological control of smooth muscle-specific gene expression through regulated nuclear translocation of serum response factor. J Bio Chem. 2000; 275:30387–93. [PubMed: 10866994]

Chai Y, Jiang X, Ito Y, Bringas P, Han J, Rowitch DH, Soriano P, McMahon AP, Sucov HM. Fate of the mammalian cranial neural crest during tooth and mandibular morphogenesis. Development. 2000; 127:1671–9. [PubMed: 10725243]

Chen EY, Huilei X, Gordonov S, Lim MP, Perkins MH, Ma'ayan A. Expression 2 Kinases: mRNA profiling linked to multiple upstream regulatory layers. Bioinformatics. 2012; 28:105–11. [PubMed: 22080467]

Choi SJ, Marazita ML, Hart PS, Sulima PP, Field LL, McHenry TG, Govil M, Cooper ME, Letra A, Menezes R, et al. The PDGF-C regulatory region SNP rs28999109 decreases promoter transcriptional activity and is associated with CL/P. Eur Journal of Hum Gen. 2009; 17:774–784.

Clark IBN, Muha V, Klingseisen A, Leptin M, Müller HAJ. Fibroblast growth factor signalling controls successive cell behaviours during mesoderm layer formation in Drosophila. Development. 2011; 138:2705–15. [PubMed: 21613323]

Cochran BH, Zullo J, Verma IM, Stiles CD. Expression of a c-fos gene and of an fos-related gene is stimulated by platelet-derived growth factor. Science. 1984; 226:1080–1082. [PubMed: 6093261]

Couly GF, Coltey PM, Le Douarin NM. The triple origin of skull in higher vertebrates: a study in quail-chick chimeras. Development. 1993; 117:409–29. [PubMed: 8330517]

Danielian PS, Muccino D, Rowitch DH, Michael SK, McMahon AP. Modification of gene activity in mouse embryos in utero by a tamoxifen-inducible form of Cre recombinase. Curr Biology. 1998; 8:1323–6.

Ding H, Wu X, Boström H, Kim I, Wong N, Tsoi B, O'Rourke M, Koh GY, Soriano P, Betsholtz C, et al. A specific requirement for PDGF-C in palate formation and PDGFR-alpha signaling. Nat Genetics. 2004; 36:1111–1116. [PubMed: 15361870]

ENCODE Project Consortium. An integrated encyclopedia of DNA elements in the human genome. Nature. 2012; 489:57–74. [PubMed: 22955616]

Esnault C, Stewart A, Gualdrini F, East P, Horswell S, Matthews N, Treisman R. Rho-actin signaling to the MRTF coactivators dominates the immediate transcriptional response to serum in fibroblasts. Genes & Dev. 2014; 28:943–58. [PubMed: 24732378]

Etchevers HC, Vincent C, Le Douarin NM, Couly GF. The cephalic neural crest provides pericytes and smooth muscle cells to all blood vessels of the face and forebrain. Development. 2001; 128:1059–68. [PubMed: 11245571]

Fambrough D, McClure K, Kazlauskas A, Lander ES. Diverse signaling pathways activated by growth factor receptors induce broadly overlapping, rather than independent, sets of genes. Cell. 1999; 97:727–41. [PubMed: 10380925]

Fantauzzo KA, Soriano P. PI3K-mediated PDGFRα signaling regulates survival and proliferation in skeletal development through p53-dependent intracellular pathways. Genes & Dev. 2014; 28:1005–1017. [PubMed: 24788519]

Fera E, O'Neil C, Lee W, Li S, Pickering JG. Fibroblast growth factor-2 and remodeled type I collagen control membrane protrusion in human vascular smooth muscle cells: biphasic activation of Rac1. J Bio Chem. 2004; 279:35573–82. [PubMed: 15166228]

Franco CA, Mericskay M, Parlakian A, Gary-Bobo G, Gao-Li J, Paulin D, Li Z. Serum response factor is required for sprouting angiogenesis and vascular integrity. Dev Cell. 2008; 15:448–61. [PubMed: 18804439]

Fuchs S, Herzog D, Sumara G, Büchmann-Møller S, Civenni G, Wu X, Chrostek-Grashoff A, Suter U, et al. Stage-specific control of neural crest stem cell proliferation by the small rho GTPases Cdc42 and Rac1. Cell Stem Cell. 2009; 4:236–47. [PubMed: 19265663]

Gerber A, Esnault C, Aubert G, Treisman R, Pralong F, Schibler U. Blood-borne circadian signal stimulates daily oscillations in actin dynamics and SRF activity. Cell. 2013; 152:492–503. [PubMed: 23374345]

Gineitis D, Treisman R. Differential usage of signal transduction pathways defines two types of serum response factor target gene. J Bio Chem. 2001; 276:24531–9. [PubMed: 11342553]

Hamilton TG, Klinghoffer RA, Corrin PD, Soriano P. Evolutionary Divergence of Platelet-Derived Growth Factor Alpha Receptor Signaling Mechanisms. Mol Cell Bio. 2003; 23:4013–25. [PubMed: 12748302]

He F, Soriano P. A critical role for PDGFRα signaling in medial nasal process development. PLoS Genetics. 2013; 9:e1003851. [PubMed: 24086166]

Ho CY, Jaalouk DE, Vartiainen MK, Lammerding J. Lamin A/C and emerin regulate MKL1-SRF activity by modulating actin dynamics. Nature. 2013; 497:507–11. [PubMed: 23644458]

Hoch RV, Soriano P. Context-specific requirements for Fgfr1 signaling through Frs2 and Frs3 during mouse development. Development. 2006; 133:663–73. [PubMed: 16421190]

Iyer D, Chang D, Marx J, Wei L, Olson EN, Parmacek MS, Balasubramanyam A, Schwartz RJ. Serum response factor MADS box serine-162 phosphorylation switches proliferation and myogenic gene programs. PNAS. 2006; 103:4516–21. [PubMed: 16537394]

Klinghoffer R, Hamilton TG, Hoch R, Soriano P. An allelic series at the PDGFαR locus indicates unequal contributions of distinct signaling pathways during development. Dev Cell. 2002; 2:103–113. [PubMed: 11782318]

Lau LF, Nathans D. Expression of a set of growth-related immediate early genes in BALB/c 3T3 cells coordinate regulation with c-fos or c-myc. PNAS. 1987; 84:1182–6. [PubMed: 3469660]

Lemmon MA, Schlessinger J. Cell signaling by receptor tyrosine kinases. Cell. 2010; 141:1117–34. [PubMed: 20602996]

Lewis AE, Vasudevan HN, O'Neill AK, Soriano P, Bush JO. The widely used *Wnt1-Cre* transgene causes developmental phenotypes by ectopic activation of Wnt signaling. Dev Bio. 2013; 379:229–34. [PubMed: 23648512]

Luxenburg C, Pasolli HA, Williams SE, Fuchs E. Developmental roles for Srf, cortical cytoskeleton and cell shape in epidermal spindle orientation. Nat Cell Bio. 2011; 13:203–14. [PubMed: 21336301]

Medjkane S, Perez-Sanchez C, Gaggioli C, Sahai E, Treisman R. Myocardin-related transcription factors and SRF are required for cytoskeletal dynamics and experimental metastasis. Nature Cell Bio. 2009; 11:257–68. [PubMed: 19198601]

Miralles F, Posern G, Zaromytidou A, Treisman R. Actin dynamics control SRF activity by regulation of its coactivator MAL. Cell. 2003; 113:329–342. [PubMed: 12732141]

Newbern J, Zhong J, Wickramasinghe SR, Li X, Wu Y, Samuels I, Cherosky N, Karlo JC, O'Loughlin B, Wikenheiser J, et al. Mouse and human phenotypes indicate a critical conserved role for ERK2 signaling in neural crest development. PNAS. 2008; 105:17115–17120. [PubMed: 18952847]

Olson EN, Nordheim A. Linking actin dynamics and gene transcription to drive cellular motile functions. Nat Rev Mol Cell Bio. 2010; 11:353–365. [PubMed: 20414257]

Park EJ, Watanabe Y, Smyth G, Miyagawa-Tomita S, Meyers E, Klingensmith J, Camenisch T, Buckingham M, Moon AM. An FGF autocrine loop initiated in second heart field mesoderm regulates morphogenesis at the arterial pole of the heart. Development. 2008; 135:3599–610. [PubMed: 18832392]

Parlakian A, Tuil D, Hamard G, Hentzen D, Concordet J, Paulin D, Li Z, Daegelen D. Targeted Inactivation of Serum Response Factor in the Developing Heart Results in Myocardial Defects and Embryonic Lethality. Mol Cell Bio. 2004; 24:5281–5289. [PubMed: 15169892]

Pipes GCT, Creemers EE, Olson EN. The myocardin family of transcriptional coactivators: versatile regulators of cell growth, migration, and myogenesis. Genes & Dev. 2006; 20:1545–56. [PubMed: 16778073]

Posern G, Treisman R. Actin' together: serum response factor, its cofactors and the link to signal transduction. Trends in Cell Biology. 2006; 16:588–96. [PubMed: 17035020]

R Core Team. R: A language and environment for statistical computing. R Foundation for Statistical Computing; Vienna, Austria: 2013.

Rattanasopha S, Tongkobpetch S, Srichomthong C, Siriwan P, Suphapeetiporn K, Shotelersuk V. PDGFRa mutations in humans with isolated cleft palate. Eur J Hum Gen. 2012; 20:1058–62.

Rivera VM, Miranti CK, Misra RP, Ginty DD, Chen RH, Blenis J, Greenberg ME. A growth factor-induced kinase phosphorylates the serum response factor at a site that regulates its DNA-binding activity. Mol Cell Bio. 1993; 13:6260–6273. [PubMed: 8413226]

Schmahl J, Raymond CS, Soriano P. PDGF signaling specificity is mediated through multiple immediate early genes. Nat Genetics. 2007; 39:52–60. [PubMed: 17143286]

Schratt G, Philippar U, Berger J, Schwarz H, Heidenreich O, Nordheim A. Serum response factor is crucial for actin cytoskeletal organization and focal adhesion assembly in embryonic stem cells. J Cell Bio. 2002; 156:737–50. [PubMed: 11839767]

Soriano P. The PDGF alpha receptor is required for neural crest cell development and for normal patterning of the somites. Development. 1997; 2700:2691–2700. [PubMed: 9226440]

Soriano P. Generalized lacZ expression with the ROSA26 Cre reporter strain. Nat Genetics. 1999; 21:70–71. [PubMed: 9916792]

Stritt C, Stern S, Harting K, Manke T, Sinske D, Schwarz H, Vingron M, Nordheim A, et al. Paracrine control of oligodendrocyte differentiation by SRF-directed neuronal gene expression. Nat Neuroscience. 2009; 12:418–27.

Sullivan AL, Benner C, Heinz S, Xie L, Miano JM, Glass CK, Huang W. Serum Response Factor Utilizes Distinct Mechanisms To Regulate Cytoskeletal Gene Expression in Macrophages Serum Response Factor Utilizes Distinct Promoter- and Enhancer-Based Mechanisms To Regulate Cytoskeletal Gene Expression. Mol Cell Bio. 2011; 31:861–875. [PubMed: 21135125]

Sun Y, Boyd K, Xu W, Ma J, Jackson CW, Fu A, Shillingford JM, Robinson GW, Hennighausen L, Hitzler JK, et al. Acute myeloid leukemia-associated Mkl1 (Mrtf-a) is a key regulator of mammary gland function. Mol Cell Bio. 2006; 26:5809–26. [PubMed: 16847333]

Tallquist MD, Soriano P. Cell autonomous requirement for PDGFRalpha in populations of cranial and cardiac neural crest cells. Development. 2003; 130:507–518. [PubMed: 12490557]

Theveneau E, Mayor R. Neural crest delamination and migration: From epithelium-to-mesenchyme transition to collective cell migration. Dev Bio. 2012; 366:34–54. [PubMed: 22261150]

Thomas PS, Kim J, Nunez S, Glogauer M, Kaartinen V. Neural crest cell-specific deletion of Rac1 results in defective cell-matrix interactions and severe craniofacial and cardiovascular malformations. Dev Bio. 2010; 340:613–25. [PubMed: 20184871]

Traverse S, Seedorf K, Paterson H, Marshall CJ, Cohen P, Ullrich A. EGF triggers neuronal differentiation of PC12 cells that overexpress the EGF receptor. Curr Biology. 1994; 4:694–701.

Treisman R. Identification and purification of a polypeptide that binds to the c-fos serum response element. EMBO Journal. 1987; 6:2711–2717. [PubMed: 3119326]

Treisman R. Regulation of transcription by MAP kinase cascades. Curr Opinion Cell Bio. 1996; 8:205–15. [PubMed: 8791420]

Trokovic N, Trokovic R, Mai P, Partanen J. Fgfr1 regulates patterning of the pharyngeal region. Genes & Dev. 2003; 17:141–153. [PubMed: 12514106]

Vartiainen MK, Guettler S, Larijani B, Treisman R. Nuclear actin regulates dynamic subcellular localization and activity of the SRF cofactor MAL. Science. 2007; 316:1749–52. [PubMed: 17588931]

Wang C, Chang JYF, Yang C, Huang Y, Liu J, You P, Li X. Type 1 fibroblast growth factor receptor in cranial neural crest cell-derived mesenchyme is required for palatogenesis. J Bio Chem. 2013; 288:22174–83. [PubMed: 23754280]

Wang Z, Wang D, Hockemeyer D, Mcanally J, Nordheim A, Olson EN. Myocardin and ternary complex factors compete for SRF to control smooth muscle gene expression. Nature. 2004; 428:185–189. [PubMed: 15014501]

Wickramasinghe SR, Alvania RS, Ramanan N, Wood JN, Mandai K, Ginty D. Serum response factor mediates NGF-dependent target innervation by embryonic DRG sensory neurons. Neuron. 2008; 58:532–45. [PubMed: 18498735]

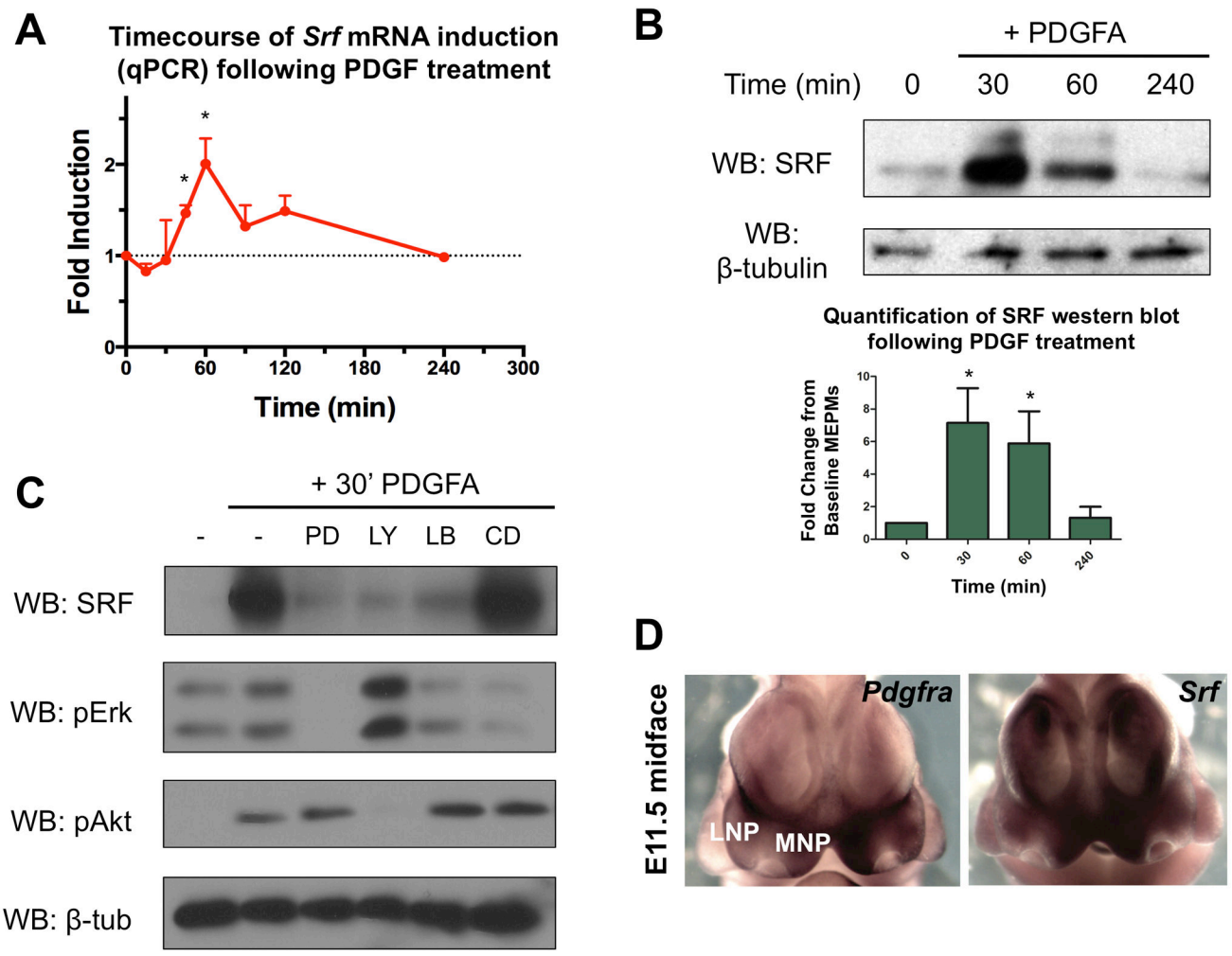

Figure 1.

SRF is a target of PDGF signaling in craniofacial development. (A–B) In E13.5 MEPMs, PDGF stimulation increases (A) *Srf* mRNA (2-fold peak induction) and (B) protein (7-fold peak induction) (n=3). Data plotted as mean ± SEM. *p<0.05. (C) SRF induction following PDGF stimulation requires ERK, PI3K, and MRTF activity, as evidenced by inhibition of these pathways. Cells treated with 30 ng/mL PDGFAA for desired duration. PD = PD325901, LY = LY294002, LB = Latrunculin B, CD = cytochalasin D. (D) At E11.5, *Pdgfra* and *Srf* mRNA are coexpressed in the developing medial nasal process (MNP) and less robustly in the lateral nasal process (LNP). See also Fig. S1 and Table S2.

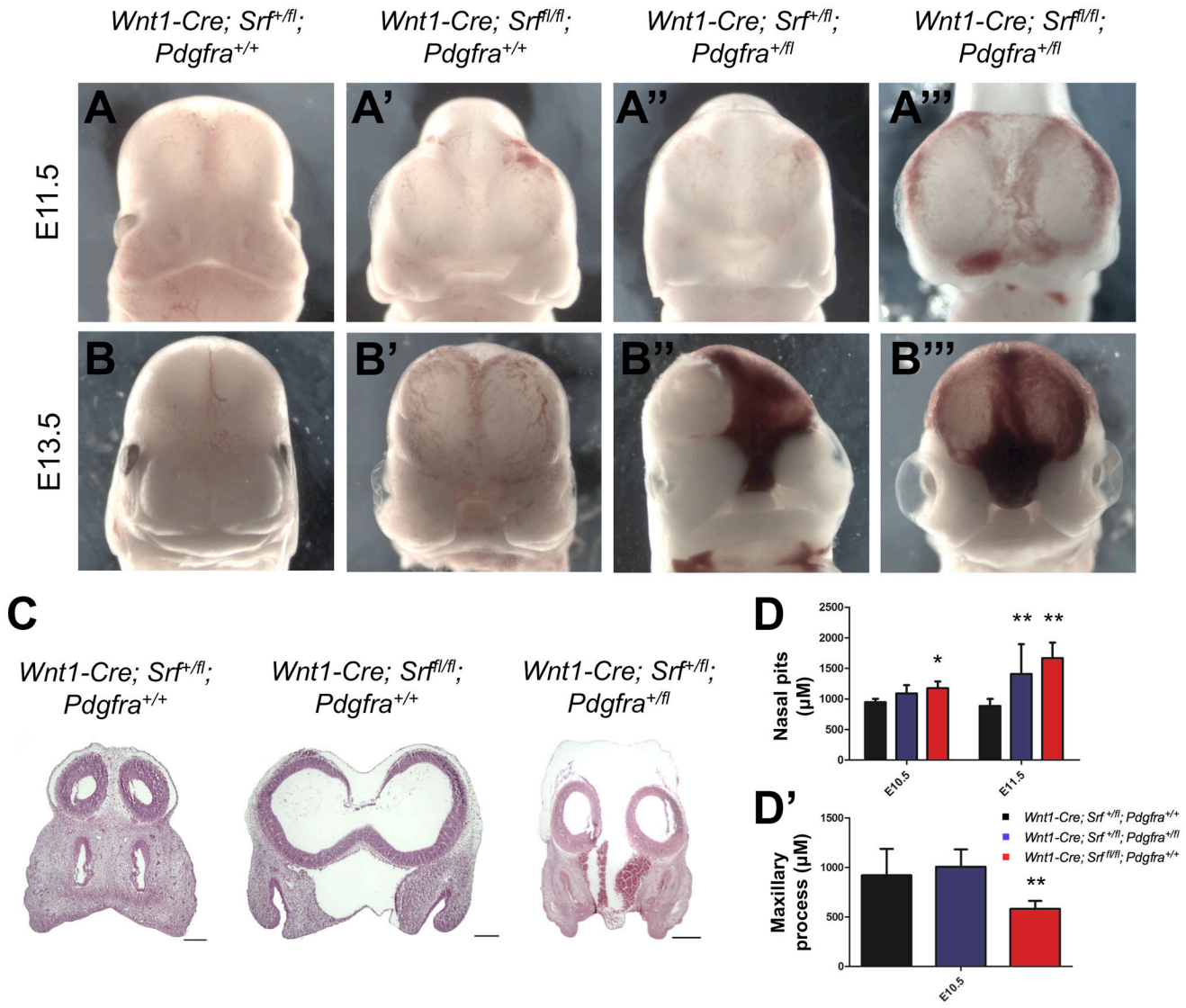

Figure 2.

Wnt1-Cre; Srf$^{fl/fl}$ mutants exhibit facial clefting and interact genetically with *Pdgfra*. (A–B) Neural crest cell conditional deletion of *Srf* results in fully penetrant facial clefting at both (A, A′) E11.5 and (B, B′) E13.5. (A″, B″) Embryos heterozygous for both *Srf* and *Pdgfra* display a partially penetrant clefting phenotype while (A‴, B‴) *Srf* homozygous mutants missing one copy of *Pdgfra* display exacerbated phenotypes, including severe midline hemorrhage and blebbing. (C) Frontal sections in E11.5 embryos show clefting and forebrain expansion in both the *Wnt1-Cre; Srf*$^{fl/fl}$ and *Wnt1-Cre; Srf*$^{+/fl}$; *Pdgfra*$^{+/fl}$ mutants as well as midline hemorrhage in the double heterozygous condition. (D) Morphometry reveals differences in the distance between nasal pits and (D′) maxillary process length in *Wnt1-Cre; Srf*$^{fl/fl}$ mutants (n=5 at E10.5, n=11 at E11.5) and *Wnt1-Cre; Srf*$^{+/fl}$; *Pdgfra*$^{+/fl}$ embryos (n=4 at E10.5, n=9 at E11.5) compared to controls (n=10 at E10.5, n=10 at E11.5). *p<0.05. **p<0.01. Scale bars: 200 μm. All data plotted as mean ± SEM. See also Fig. S2 and Table S1.

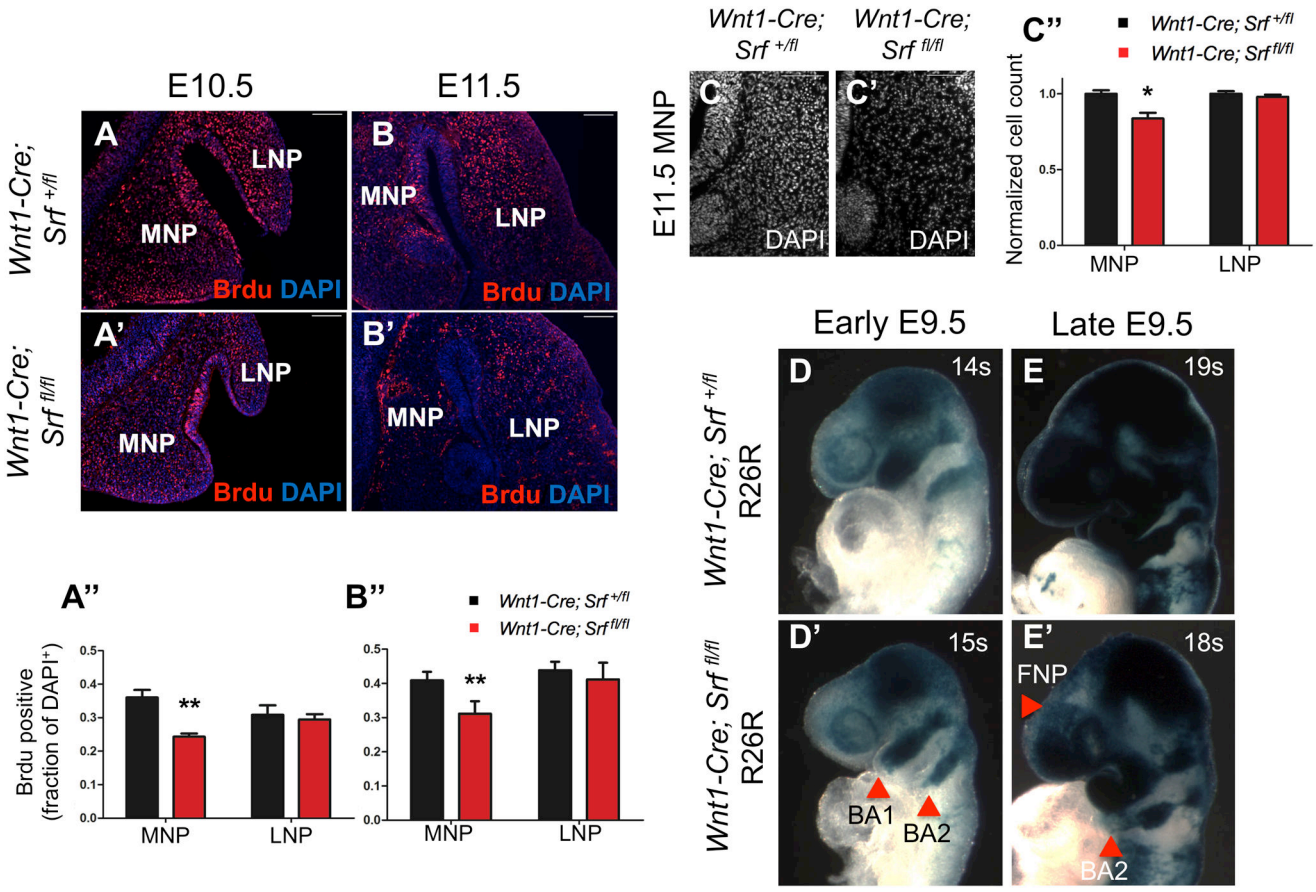

Figure 3.

Wnt1-Cre; Srf$^{fl/fl}$ mutants display proliferation and lineage tracing defects *in vivo*. (A, B) *Srf* mutants exhibit decreased proliferation specifically in the MNP at (A-A″) E10.5 (n=5) and (B-B″) E11.5 (n=7). **p<0.001. (C) The MNP of *Srf* conditional mutants is hypocellular, with significantly fewer cells at E11.5 (n=7). Cell counts were normalized to number of cells in littermate control. *p<0.005. (D, E) Lineage tracing using the ROSA26 reporter (R26R) reveals reduced contribution of neural crest cells to (D, D′) the first and second branchial arches (BA1, BA2) and (E, E′) frontonasal prominence (FNP) at E9.5 (somite number indicated). Blue (lacZ positive) cells are generated by Wnt1Cre mediated recombination and thus label the neural crest and its derivatives. Scale bars: 100 μm. All data plotted as mean ± SEM.

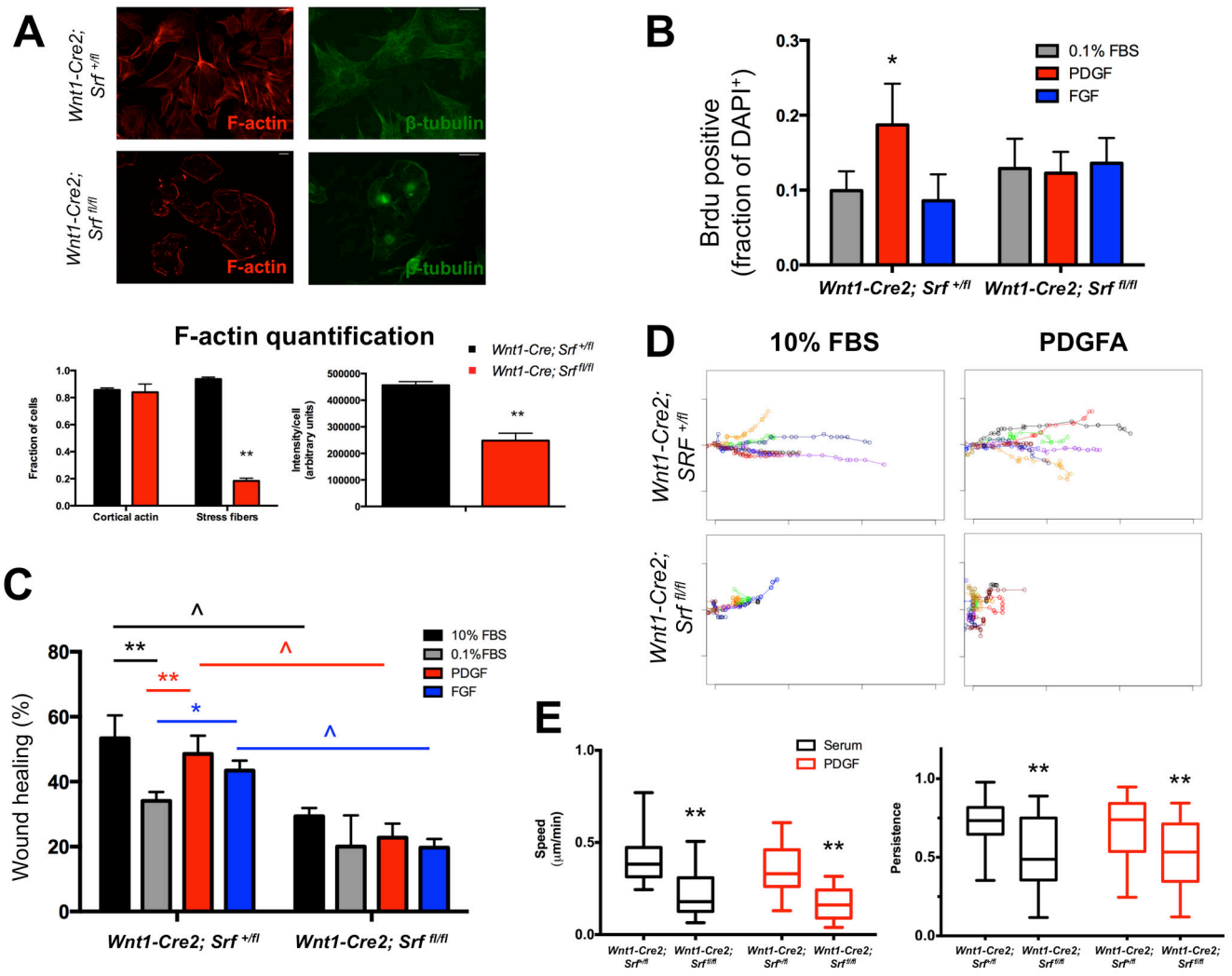

Figure 4.

Srf mutant E11.5 facial prominence cells (FPCs) do not proliferate in response to PDGF and exhibit defective wound healing. (A) *Srf* mutant FPCs lack actin stress fibers, show decreased total F-actin staining, and display gross microtubule disorganization. (n>100 cells/condition) (B) Control FPCs exhibit a modest proliferative response to PDGF stimulation, but *Srf* mutant FPCs fail to proliferate in response to PDGF (n=4). (C) Although control FPCs show significant wound healing when treated with 10% FBS, PDGF, or FGF compared to 0.1% FBS, *Srf* mutant FPCs fail to show significant closure when compared to 0.1% FBS starved cells (n=3). Further, *Srf* mutant FPCs show significant decreases in wound healing across all growth factor conditions when compared to control FPCs. (D) Representative trajectories from 10 cells tracked during wound healing in response to either 10% FBS or PDGF. *Srf* mutant FPCs show both decreased directionality and total distance traveled, although some mutant cells move relatively efficiently (blue trajectory in 10% FBS condition). The heterogeneous migration properties were not due to incomplete loss of SRF (Fig. S3B–C). (E) *Srf* mutant cells show decreased speed and persistence in response to both 10% FBS and PDGF when compared to control cells (quartile plot with whiskers spanning

5%–95%). Scale bars: 25 μm. Data in A–C plotted as mean ± SEM. **p<0.001. ^p<0.001. *p<0.05. Cells treated with either 30 ng/mL PDGFAA or 50 ng/mL FGF1 + 1 μg/mL heparin. See also Fig. S3.

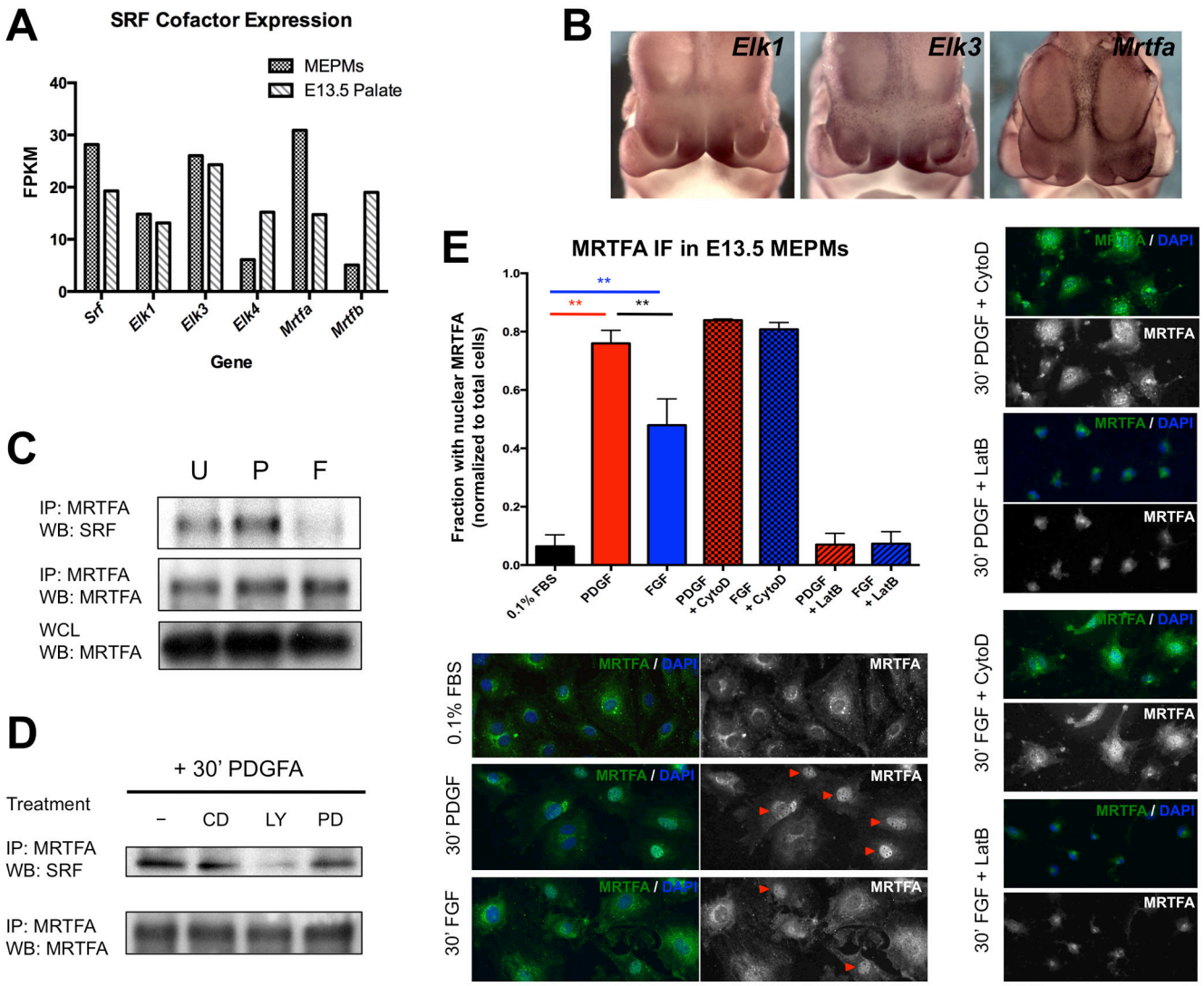

Figure 5.

Both MRTF and TCF cofactors play roles downstream of RTK signaling in craniofacial development. (A) Of the five major TCF and MRTF cofactor family members, only *Elk1*, *Elk3*, and *Mrtfa* are expressed above a threshold of 10 fragments per kilobase of transcript per million mapped reads (FPKM) in both E13.5 MEPMs and E13.5 palate. (B) Whole mount in situ hybridization reveals *Elk1* and *Elk3* mRNA are enriched in the E11.5 medial nasal process (MNP). *Mrtfa* mRNA expression in the midface is more diffuse but shares expression domains with *Pdgfra* and *Srf*. (C) PDGF modestly increases SRF-MRTFA association while FGF reduces SRF-MRTFA complex formation. MRTFA levels are not modulated by PDGF or FGF treatment, thus serving as an additional loading control. (D) MRTFA-SRF association following 30 minutes PDGF stimulation requires PI3K activity. All biochemistry performed in E13.5 MEPMs. CD = cytochalasin D, PD = PD325901, LY = LY294002. U = untreated cells, P = 30 minutes 30 ng/mL PDGFAA, F = 30 minutes 50 ng/mL FGF1 + 1 μg/mL heparin. (E) MRTFA immunofluorescence shows greater nuclear accumulation of MRTFA in response to PDGF compared to FGF, although a significant

number of FGF treated cells contain nuclear MRTFA. Red arrowheads mark cells counted as containing nuclear MRTFA. Cytochalasin D and Latrunculin B were used as a positive and negative control, respectively. ** $p < 0.05$. Data plotted as mean ± SEM. See also Fig. S4.

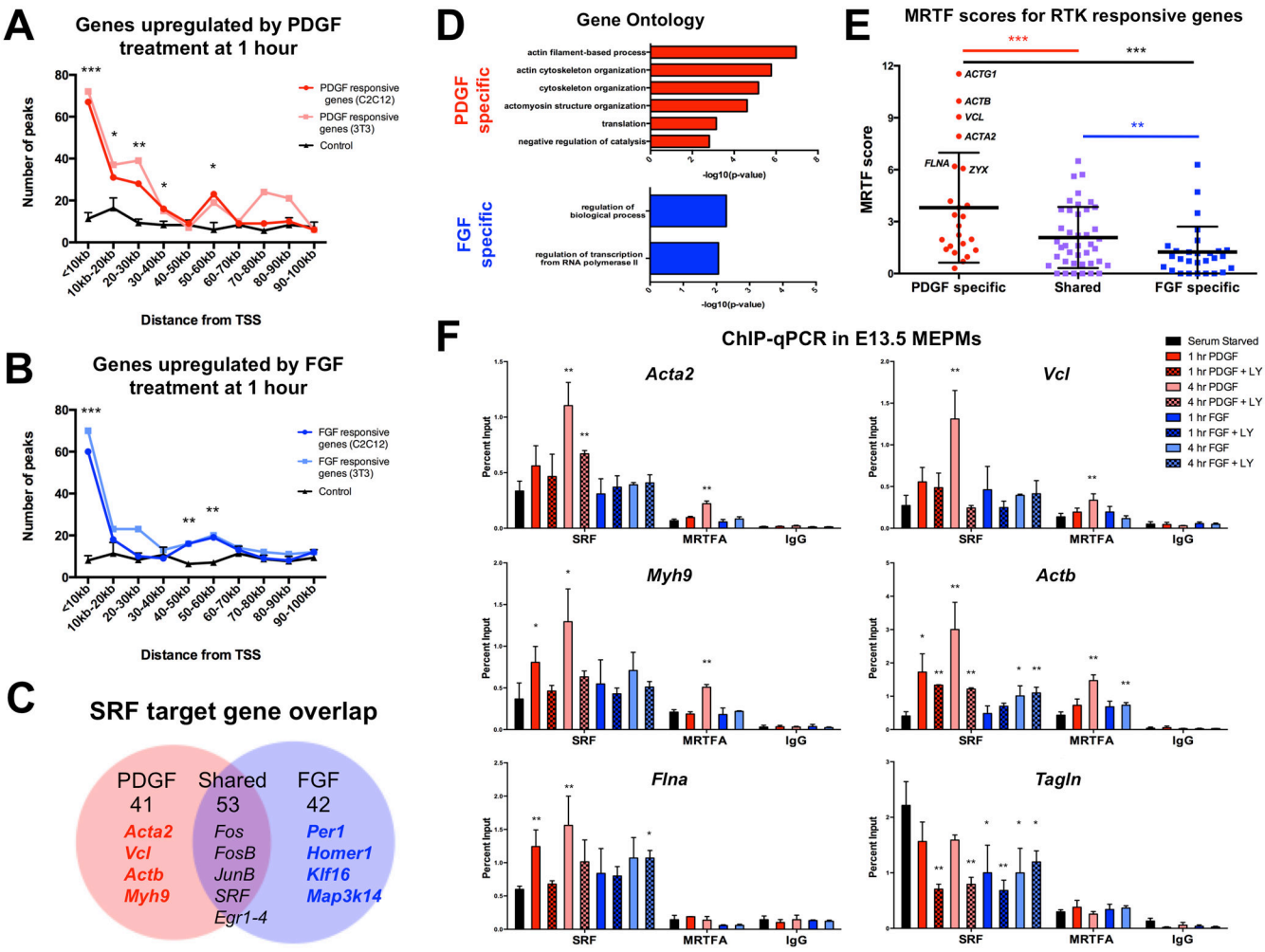

Figure 6.

Both PDGF and FGF responsive genes correlate with SRF binding genome-wide, but only PDGF target gene promoters are enriched for MRTF. (A, B) Both PDGF (red) and FGF (blue) responsive genes show enrichment for SRF binding events from C2C12 (ENCODE 2012) and 3T3 (Esnault et al. 2014) SRF ChIP-seq data. Randomly sampled expression matched control genes (black, n=3 random sets) show no such enrichment. A total of 67 PDGF responsive genes have an SRF ChIP-seq peak within 10 kb of the TSS while 52 FGF responsive genes have an SRF ChIP-seq peak within 10 kb of the TSS. *p<0.1, **p<0.05, ***p<0.01. (C) Closer inspection of SRF target genes downstream of each RTK reveals 56% overlap, with many classic IEGs (*Fos*, *Jun*, *Egr*) activated jointly by both PDGF and FGF. (D) PDGF-SRF targets show enrichment for actin cytoskeletal elements while FGF-SRF targets show minimal functional organization. (E) PDGF-SRF targets show significantly increased MRTF scores compared to FGF-SRF targets, consistent with PDGF-specific activation of an MRTF associated transcriptional program. (F) SRF and MRTFA ChIP-qPCR in E13.5 MEPMs reveals increased binding of these factors at the promoters of cytoskeletal genes in response to PDGF (red) in contrast to FGF (blue). Inhibition of PI3K signaling (patterned bars) reduces PDGF stimulated SRF binding, although a significant

response is still observed at some promoters. *p<0.1, **p<0.05, compared to serum starved. (n=3). Cells treated with 30 ng/mL PDGFAA or 50 ng/mL FGF1 + 1 μg/mL heparin. See also Fig. S5 and Table S3.

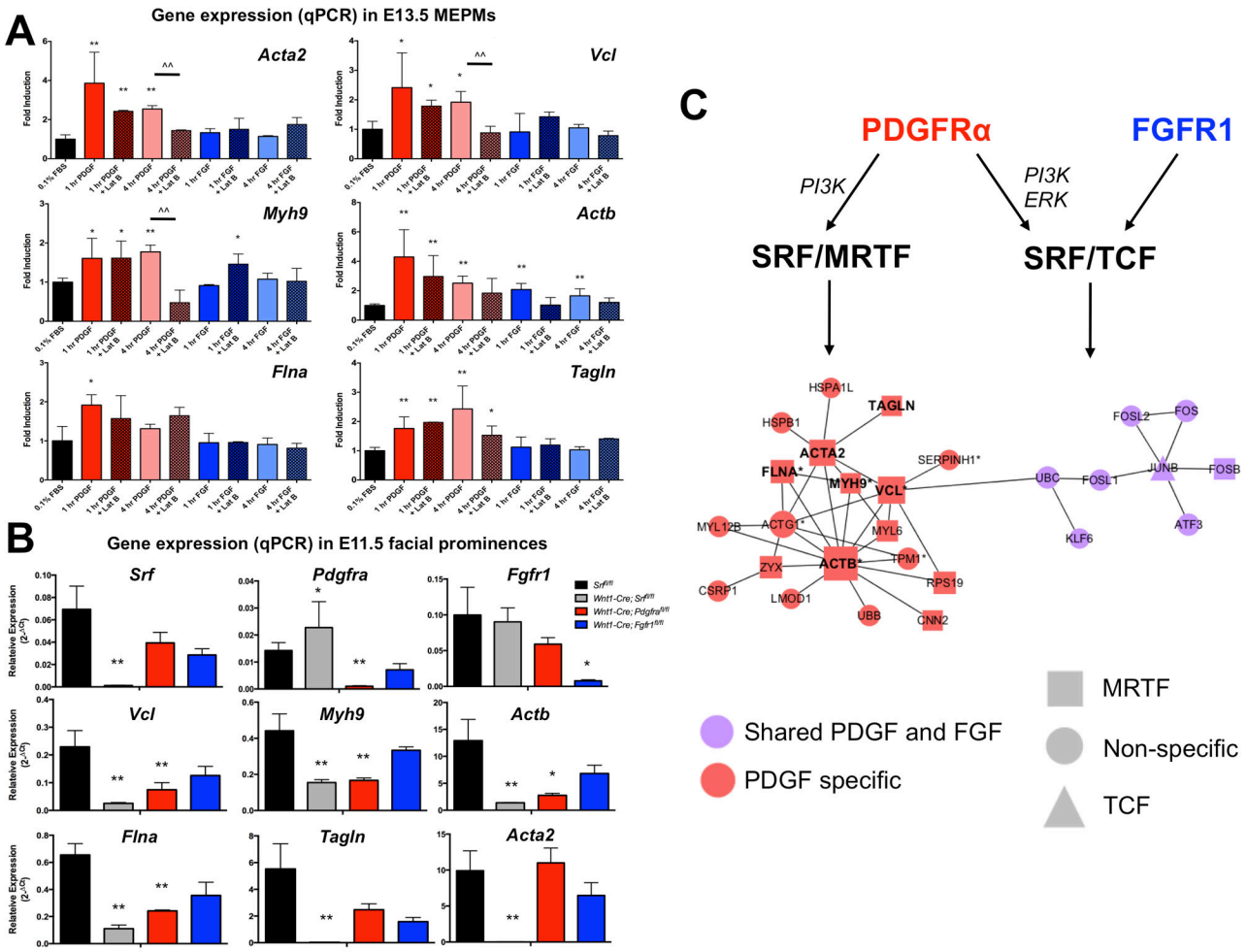

Figure 7.

A PDGF-MRTF-SRF axis controls expression of key cytoskeletal regulators in craniofacial development.. (A) PDGF (red bars) robustly activates expression of cytoskeletal target genes in MEPMs while FGF (blue bars) does not. Latrunculin B treatment (patterned bars) inhibits PDGF mediated gene expression, indicating induction of these shared PDGF-SRF targets is MRTF dependent. (B) The expression of all six cytoskeletal SRF target genes is reduced in E11.5 *Wnt1-Cre; Srf*$^{fl/fl}$ mutant facial prominences (grey bars). While none of these genes show reduced expression in *Wnt1-Cre; Fgfr1*$^{fl/fl}$ mutant facial prominences (blue bars), four of six genes (*Vcl, Myh9, Actb*, and *Flna)* show downregulation in *Wnt1-Cre; Pdgfra*$^{fl/fl}$ mutant facial prominences (red bars). (C) Protein-protein interaction (PPI) network constructed from PDGF regulated SRF target genes (red) and FGF regulated SRF target genes (purple) recapitulates unique SRF functions downstream of PDGF signaling. Furthermore, the PDGF specific SRF network contains an enrichment of MRTF target genes (squares) compared to the shared network, which has equal TCF (triangle), MRTF (square), and non-specific (circles) genes. All six genes with altered expression in SRF mutants (bold) fall under the PDGF specific network, and many PDGF-SRF target genes have known roles in craniofacial development (* asterisk; Source: www.informatics.jax.org, www.omim.org). Data plotted as mean ± SEM. *p<0.1, **p<0.05 compared to serum starved or wildtype

control, ^^p<0.05 compared to Latrunculin B treatment (n=3). See also Fig. S6 and Table S4.